Weierstraß-Institut

für Angewandte Analysis und Stochastik

Leibniz-Institut im Forschungsverbund Berlin e. V.

Preprint ISSN 0946 – 8633

Spontaneous motion of cavity solitons induced by a delayed feedback

Mustapha Tlidi [1], Etienne Averlant [1,2] Andrei G. Vladimirov [3], Krassimir Panajotov [2,4]

submitted: September 17, 2012

[1] Faculté des Sciences
Service de Physique Mathématiques,
CP 231, Campus Plaine,
B-1050 Brussels, Belgium
E-mail: mtlidi@ulb.ac.be
Etienne.Averlant@ulb.ac.be

[2] Department of Applied Physics and Photonics (IR-TONA)
Vrije Unversiteit Brussels
Pleinlaan 2
B-1050 Brussels, Belgium
E-mail: kpanajot@b-phot.org

[3] Weierstrass Institute
Mohrenstrasse 39, D - 10117 Berlin, Germany
E-Mail: Andrei.Vladimirov@wias-berlin.de

[4] Institute of Solid State Physics
72 Tzarigradsko Chaussee Blvd.
1784 Sofia, Bulgaria

No. 1737

Berlin 2012

2010 *Mathematics Subject Classification.* 78A60, 37L10.

2010 *Physics and Astronomy Classification Scheme.* 05.45.-a, 02.30.Ks, 42.65.-k.

Key words and phrases. semiconductor lasers, delayed feedback, Swift-Hohenberg equation, localized structures, bifurcations.

Fruitful discussions with Svetlana Gurevich are gratefully acknowledged. A.G.V. was supported by SFB 787 of the DFG, EU FP7 ITN PROPHET, Grant No. 264687, Walton Award of the SFI, and the grant 2011-1.5-503-002-038 of MES of Russia. M.T received support from the FNRS (Belgium). This research was supported by the IAP program of the BELSPO, under grant IAP P7-35 “photonics@be”.

Edited by
Weierstraß-Institut für Angewandte Analysis und Stochastik (WIAS)
Leibniz-Institut im Forschungsverbund Berlin e. V.
Mohrenstraße 39
10117 Berlin
Germany

Fax: +49 30 20372-303
E-Mail: preprint@wias-berlin.de
World Wide Web: http://www.wias-berlin.de/

Abstract

We consider a broad area Vertical-Cavity Surface Emitting Laser (VCSEL) operating below the lasing threshold and subject to optical injection and time-delayed feedback. We derive a generalized delayed Swift-Hohenberg equation for the VCSEL system which is valid close to the nascent optical bistability. We first characterize the stationary cavity solitons by constructing their snaking bifurcation diagram and by showing clustering behavior within the pinning region of parameters. Then we show that the delayed feedback induces a spontaneous motion of two-dimensional cavity solitons in an arbitrary direction in the transverse plane. We characterize moving cavity solitons by estimating their threshold and calculating their velocity. Numerical 2D solutions of the governing semiconductor laser equations are in close agreement with those obtained from the delayed generalized Swift-Hohenberg equation.

1 Introduction

During the last two decades, the study of localized structures, often called dissipative solitons or cavity solitons (CSs), has attracted considerable attention in many area of natural science such as chemistry, plant ecology, and optics (see recent overviews, [1]-[5]). They attract growing interest in optics due to potential applications for all-optical control of light, optical storage, and information processing [6]-[12]. These stable localized objects arise in dissipative environment and belong to the class of dissipative structures found far from equilibrium. Cavity solitons are stationary localized intensity peaks that appear in a subcritical regime involving a homogeneous background of radiation and a self-organized periodic pattern which are both linearly stable. They can be manipulated individually by the process of writing or erasing through an external control beam when they are sufficiently well separated from each other. When, however, the distance between peaks decreases they start to interact through their oscillating, exponentially decaying tails. This interaction then leads to the formation of clusters. Therefore, the number of peaks and their spatial distribution in the transverse plane can be either independent and randomly distributed or clustered forming a well defined spatial pattern [13]. Recently, the relative stability analysis of different clusters of closely packed localized peaks has been performed [14].

Cavity solitons are not necessary stationary objects. They can be time dependent, e.g. moving or oscillating. In particular, different mechanisms leading to the motion of dissipative solitons have been described in the literature. It has been shown that uniform motion of solitons can be induced by a vorticity [15], a finite relaxation rates [16, 17, 18], a phase gradient [19], an Ising-Bloch transition [20, 21, 22], a walk-off, a symmetry breaking due to off-axis feedback [23], a resonator detuning [24], or a Hopf-Turing interacting bifurcations [25].

More recently, it has been shown that inclusion of delayed feedback in the dynamics of spatially extended systems can lead to a drift instability of cavity solitons [26]. This behavior has been identified first in the case when the delayed feedback is frequency selective [28]-[31]. Spontaneous motion of a single cavity soliton in the case of non-frequency selective (i.e., regular) feedback has been predicted in [26]. This result has been obtained with a model of passive nonlinear cavity filled with two-level atoms without population inversion and driven coherently by an external injected beam. Other studies of various spatially extended systems with time delay have motivated further to investigate this subject [32].

In this paper, we investigate the effect of a regular delayed feedback on the mobility properties of 2D cavity solitons in a broad area Vertical-Cavity Surface-Emitting Laser (VCSEL). The delayed feedback is provided by an external mirror located at a distance L from the output facet of the VCSEL. The structure of the considered device is schematically illustrated in Fig. 1. We assume that the laser operates in a single-longitudinal mode, the diffraction in the external cavity is fully compensated, and the feedback field is sufficiently attenuated, so that it can be modeled by a single delay term with a spatially homogeneous coefficient. We show that this device can admit both stationary dissipative solitons and solitons moving in the transverse direction. Unlike previous communication where the analysis is performed in strictly one transverse dimension [33] here we consider the case of two transverse dimensions. We show that stationary cavity solitons exhibit a clustering behavior which has been experimentally observed in [34]. This behavior corresponds to back and forth oscillations of the laser output energy curve inside the pinning region. We explore the mechanism of formation of localized structures by constructing their bifurcation diagram with changing amplitude of optical injection. We show that when the strength of the delayed feedback exceeds some threshold value two-dimensional cavity solitons exhibit a spontaneous motion in the laser transverse section.

The paper is organized as follows: in section II, we introduce and discuss the VCSEL model. In section III, in the neighborhood of the second-order critical point marking the onset of hysteresis loop, we derive the generalized Swift-Hohenberg equation with time delay and perform linear stability analysis of the spatially homogeneous stationary solutions of this equation. In section IV, we describe the snaking bifurcation diagram associated with stationary cavity solitons. Analytical calculations of the drift instability threshold as well as the velocity of moving solitons are obtained in this section. Finally, numerical simulations of the generalized Swift-Hohenberg equation with time delay are presented in section IV together with the results of numerical integration on the original laser model. Concluding remarks are given in section V.

2 Mean field model of VCSEL with time delay

The laser model under consideration is obtained from the scalar Maxwell-Bloch equations using the slowly varying envelope and paraxial approximations. We assume that the laser operates in a single longitudinal mode. Under these approximations, the mean field model describing the space-time evolution of the electric field envelope E and the normalized carrier density Z in a broad area VCSEL subject to optical injection and delayed optical feedback is given by the

following set of dimensionless partial differential equations [33]

$$\begin{aligned} \partial_{t'} E &= -(1+i\theta)\, E + 2C(1-i\alpha)(Z-1)E \qquad (1) \\ &+ E_i + \xi e^{i\psi} E(t'-\tau') + i\nabla_\perp'^2 E \\ \partial_{t'} Z &= -\gamma' \left[Z - I + (Z-1)\,|E|^2 - d\nabla_\perp'^2 Z \right] \qquad (2) \end{aligned}$$

where E_i is the amplitude of the injected beam. The parameter θ is the cavity detuning, C is the bistability parameter, and α is the linewidth enhancement factor. The delayed feedback is characterized by three parameters: feedback strength ξ, feedback phase ψ, and time delay τ'. The parameter γ' is the carrier decay rate, I is the injected current (we assume that the laser operates below the lasing threshold), and d is the diffusion coefficient. The diffraction of light and diffusion of the carriers are described by the Laplace operator $\nabla_\perp'^2 = \partial^2_{x'x'} + \partial^2_{y'y'}$ acting of the transverse plane (x', y'). In the absence of delayed feedback, $\xi = 0$, we recover the mean field model of Ref. [35]. The linear stability analysis of the spatially homogeneous steady states of Eqs. (1) and (2) as well as numerical analysis of stationary and moving cavity solitons have been performed in [33] in strictly one dimensional setting.

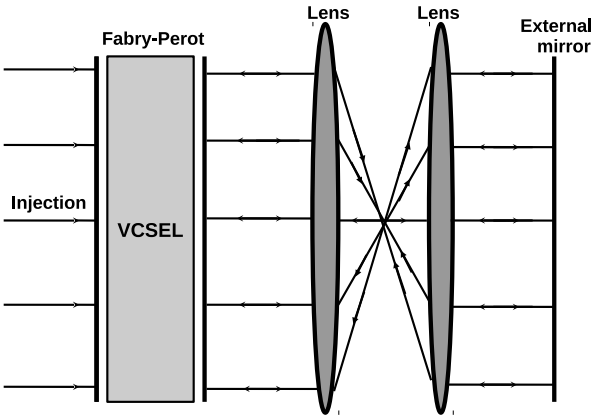

Figure 1: Schematic setup of a Fabry-Perot cavity with delayed optical feedback and driven by a coherent external injected beam. The nonlinear medium consists of a vertical-cavity surface emitting laser. To compensate the diffraction in the external cavity we use two lenses in self-imaging configuration.

In order to reduce the number of free parameters, we introduce the following change of variables: $n = [2C(Z-1)-1]/2$ and $e = E^*/\sqrt{2}$. The model equations (1,2) of semiconductor laser driven by an injected field $Y = E_i/(2\sqrt{2})$ take the following form:

$$\begin{aligned} \partial_t e &= i\theta' e + (1+i\alpha) n e + Y + \eta' e^{-i\psi} e(t-\tau) - i\nabla_\perp^2 e \qquad (3) \\ \partial_t n &= \gamma[P - n - (1+2n)|e|^2 + D\nabla_\perp^2 n] \qquad (4) \end{aligned}$$

The pump parameter P is $P = C(I-1) - 1/2$, $\gamma = \gamma'/2$, $D = 2d$, $\eta' = \xi/2$, and $\theta' = (\theta+\alpha)/2$. The new time and space scales are $(t, \tau) = 2(t', \tau')$ and $\nabla_\perp^2 = 2\nabla_\perp'^2$. Let us assume for simplicity that the detuning and the feedback phase are zero in the model

equations (3) and (4), i.e., $\theta' = 0$ and $\psi = (0, \pi)$. The homogeneous steady states are solutions of the two coupled equations $Y = -e_s(1 + i\alpha)(P - |e_s|^2)/(1 + 2|e_s|^2)$ and $n_s = (P - |e_s|^2)/(1 + 2|e_s|^2)$. It is well known that the dynamics of a driven semiconductor cavity exhibits Turing instability and hysteresis, the former giving rise to either periodic or localized patterns consisting of localized intensity pulses in the transverse plane. In order to obtain a qualitative picture of the dynamics of this system, we focus our analysis on regime which is (i) close to the nascent bistability threshold where the phenomenon of slowing down occurs, i.e., $\partial Y/\partial|e_s| = \partial^2 Y/\partial|e_s|^2 = 0$, and (ii) close to long wavelength pattern forming instability. In this regime, the space-time dynamics is governed by the well know Swift-Hohenberg equations [36].

3 Derivation of the generalized Swift-Hohenberg equation with time delay

In this section we explore, the nascent optical bistability regime near the critical point where the output intensity as a function of the injection parameter Y has an infinite slope, i.e., $\partial Y/\partial|e_s| = \partial^2 Y/\partial|e_s|^2 = 0$. The coordinates of the critical point are $e_c = (1 - i\alpha)\sqrt{3/2(1 + \alpha^2)}$, $n_c = -3/2$, $P_c = -9/2$, $D_c = 8\alpha/[3(1 + \alpha^2)]$ and $Y_c = (3/2)^{(3/2)}(1 + \alpha^2)^{1/2}$. We consider large time delay regime and we assume that the amplitude of the feedback strength is small: $\eta' = \eta\varepsilon^2$ and $\tau \to (1/\gamma + D_c/\alpha)\tau\varepsilon^2$, where ε is a small parameter and $\eta, \tau = \mathcal{O}(1)$. We seek corrections to the steady state solution at the criticality that depend on time and space via the slow variables $t \to (1/\gamma + D_c/\alpha)\varepsilon^2 t$ and $(x, y) \to (\varepsilon/D_c)^{1/2}(x, y)$. We expand the input field amplitude Y, the parameter P, and the variables e and n around their critical values, $e = e_c(1 + \varepsilon u + \varepsilon^2 e_2...)$, $n = n_c(1 + \varepsilon n_1 + \varepsilon^2 n_2...)$, $Y = Y_c(1 - \varepsilon^2 p_2/2 + \varepsilon^3 y...)$, $P = P_c(1 + 3\varepsilon^2 p_2 + ...)$, and $D = D_c(1 + \varepsilon d + ...)$. We substitute these expansions and the space-time scalings in Eqs. (3) and (4). We get $u = -n_1$ in the leading order problem, i.e., $\mathcal{O}(\epsilon)$ where u has to be real. At the $\mathcal{O}(\epsilon^2)$, we obtain $e_2 = -i[\nabla_\perp^2 u/(4\alpha) + 2\eta\alpha/(3(1+\alpha^2))]$ and $n_2 = u^2 - p_2/2 - \nabla_\perp^2 n_1/4$. Finally the solvability condition at $\mathcal{O}(\epsilon^3)$ leads to the following delayed partial differential equation

$$\begin{aligned} \partial_t u &= y - u(p + u^2) + \eta u(t - \tau) \\ &+ (d - \frac{5u}{2})\nabla_\perp^2 u - a\nabla_\perp^4 u - 2(\nabla_\perp u)^2, \end{aligned} \tag{5}$$

where $a = (1 - \alpha^2)/(4\alpha^2)$. Note that y is the deviation from the injected field amplitude and transverse coordinate at the same time. The real variable u, the parameters p and d are the deviations of the electric field, the pump parameter and the carrier diffusion coefficient from their values at the onset of the critical point, respectively. In the absence of delay; i.e., $\eta = 0$, Eq. (5) is the generalized Swift-Hohenberg equation that has been derived for many far from equilibrium systems [36, 37]. Equation (5) model differs from the usual delayed Swift-Hohenberg equation [26, 37] in two significant ways. First, the presence of nonlinear diffusion terms $u\nabla_\perp^2 u$ breaks the symmetry $u \mapsto -u$ and allows Eq. (5) to exhibit modulational instabilities with different wavelengths. Second, in the absence of delay the equation (5) is nonvariational devoid of gradient form, and therefore it does not admit a Lyapunov functional or a free energy to

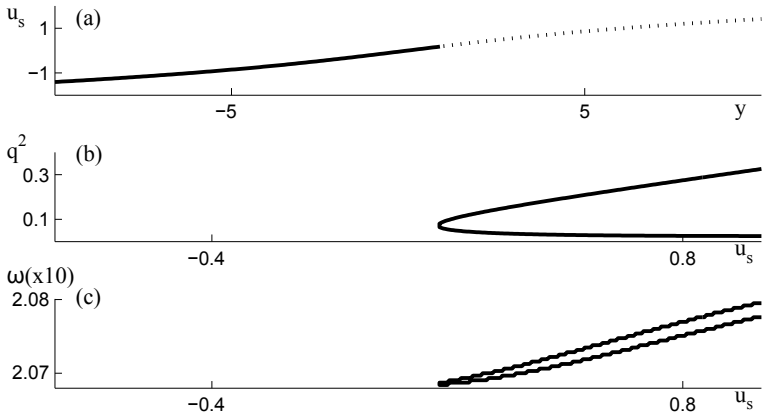

Figure 2: Stability curves associated with traveling wave instability in the monostable regime. The characteristics: (a) output field (u_s) as a function of input field (y); (b) wavenumber q^2 and (c) angular frequency ω are plotted as a function of output field (u_s). The full and the broken lines correspond, respectively, to stable and unstable homogeneous steady states. Parameters are $p = 5$, $d = -1$, $a = 0.1$, $\eta = -0.1$, and $\tau = 15$.

minimize. As a consequence, cavity soliton could move with a constant velocity even in absence of delayed feedback [37].

The homogeneous stationary solutions u_s of Eq. (5) are given by $y = u_s(p - \eta + u_s^2)$. For $p < \eta$ ($p > \eta$) the transmitted intensity as a function of the input intensity is monostable (bistable). We now perform the linear stability analysis of the homogeneous steady states. The linear deviation from the steady state is proportional to $\exp(\lambda t + i\mathbf{q}.\mathbf{r})$, where $\mathbf{r} = (x, y)$ stands for the transverse coordinates and the transverse wavevector is $\mathbf{q}$. The transcendental characteristic equation reads:

$$\lambda = -(p + 3u_s^2) - q^2(d - \frac{5u_s}{2}) - \frac{(1-\alpha^2)}{4\alpha^2}q^4 + \eta e^{-\lambda\tau} \tag{6}$$

Modulational instabilities correspond to the occurrence of zero real root ($\lambda = 0$) and $\partial_q\lambda = 0$. Our calculations show that there can be zero, one or two modulational instabilities. The critical wavenumber associated with both instabilities are:

$$q_{T\pm}^2 = \frac{\alpha^2(5u_{T\pm} - 2d)}{(1-\alpha^2)} \tag{7}$$

The threshold; $u_{T\pm}$; associated with these instabilities are:

$$u_{T\pm} = \frac{2[5\alpha^2 d \pm \sqrt{(1-\alpha^2)[\alpha^2(12d^2-37)+12](p-\eta)}]}{12 - 37\alpha^2} \tag{8}$$

Classification of different scenarios leading to the instability of the homogeneous steady state are summarized in [38].

The linear stability analysis shows that there exists a Hopf bifurcation with a finite wavenumber often called traveling wave instability. This instability occurs if a pair of complex conjugate roots

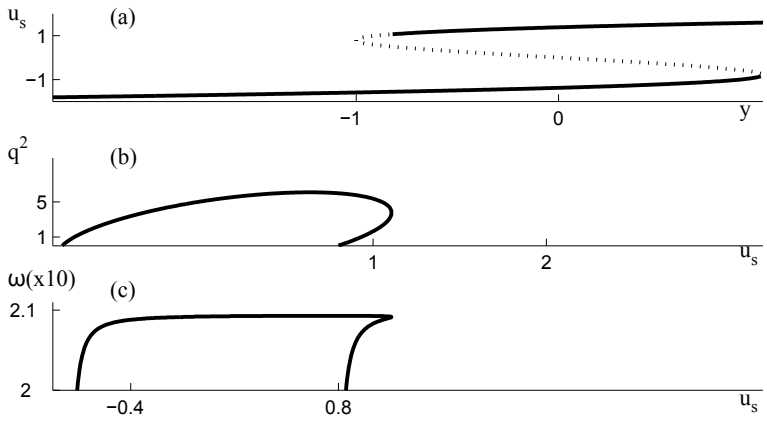

Figure 3: Stability curves associated with traveling wave instability in the monostable regime. The characteristics: (a) output field (u_s) as a function of input field (y); (b) wavenumber q^2 and (c) angular frequency ω are plotted as a function of output field (u_s). The full and the broken lines correspond, respectively, to stable and unstable homogeneous steady states. Parameters are $p = -2$, $d = -1$, $a = 2$, $\eta = -0.1$, and $\tau = 15$.

of Eq. (6) has a vanishing real part and non zero imaginary part, i.e., $\lambda = \pm i\omega$. This instability occurs when

$$\eta \cos(\omega\tau) = (3u^2 + p) + (d - \frac{5u}{2})q^2 + aq^4 \quad (9)$$

$$\eta \sin(\omega\tau) = -\omega \quad (10)$$

Two examples of stability curves are shown in Figs. 2 and 3 where we plot the homogeneous steady states in the monostable and in the bistable regimes; the unstable wavenumbers and the unstable frequencies associated with the traveling wave instability.

4 Stationary and moving localized structures

4.1 Light clustering and moving cavity solitons

In the case of one spatial dimension stationary dissipative solitons correspond to the solutions of the Swift-Hohenberg equation homoclinic in space and stationary in time. The existence of an infinite set of homoclinic solutions in the variational Swift-Hohenberg has been demonstrated [39]. This behavior is referred to as homoclinic snaking phenomenon [40]: the system exhibits a high degree of multistability in a finite range of parameters often called the pinning region. In this region, stable homogeneous steady state coexists with stable spatially periodic solution and there is an infinite set of patterns comprising different number of cavity solitons. Each of them is characterized by either odd or even number of peaks. The configuration that maximizes the number of cavity solitons in the pattern corresponds to spatially periodic distribution of the field amplitude. Examples of localized patterns having odd and even number of peaks are shown in Fig. 4. All localized patterns shown in these figures are obtained for the same parameter values and differ only by the initial condition. In the pinning region, the wavelength of the localized

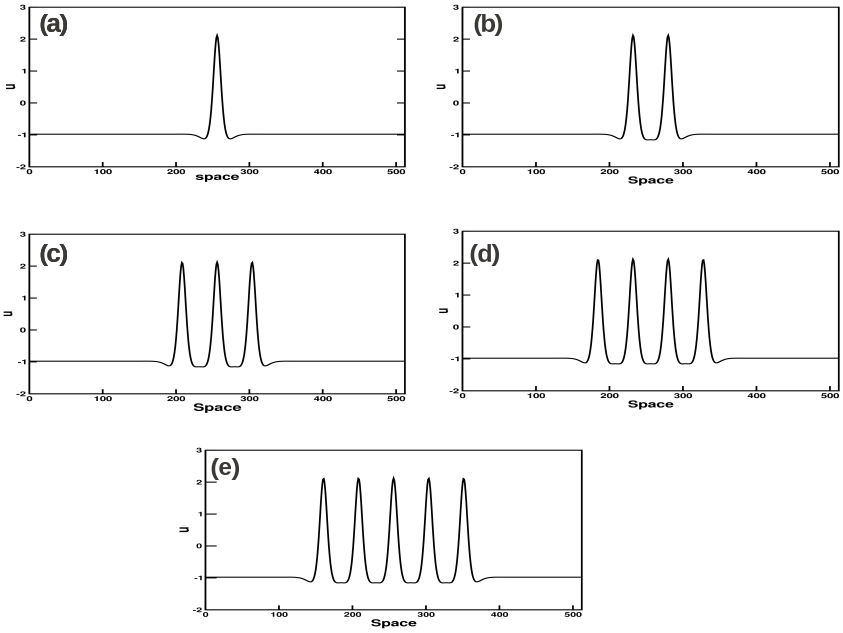

Figure 4: Stationary localized patterns formed with 1, 2, 3, 4 , and 5 cavity solitions in the amplitude of intracavity field. The parameters are $y = -0.35, p = -0.7, d = -1.2, a = 0.75$, $\tau = 1.$, and $\eta = 0.1$

patterns is close to that of the periodic structure, i.e., $\lambda_{T+} \approx 2\pi/q_{T+}$. Since the peak amplitudes of localized patterns comprising different number of solitons are close to each other, it is convenient to plot the "L_2 -norm"defined by the relation $N = \int dx|u - u_s|^2$ instead of the peak amplitudes. Typical bifurcation diagram illustrating the dependence of N on the input field amplitude y is shown in Fig. 5. It consists of two snaking curves: one corresponding to localized patterns with odd number of peaks and the other – to patterns with even number of peaks. The two inter-weaved snaking curves emerge from the modulation instability point located at $u = u_{T+}$. For each curve, as $\mathbf{N}$ increases, at every turning point where the slope becomes infinite, a pair of additional peaks appear in the pattern. It is seen from Fig. 5 that this growth is associated with back and forth oscillations around the pinning region. In the case of a fiber ring resonator, diffraction is replaced by chromatic dispersion. In this context, localized structures are often called temporal cavity solitons, which can also exhibit homoclinic snaking phenomenon [41].

In the absence of feedback all localized patterns involving odd or even numbers of cavity solitons are stationary. As we shall see in the next subsection, when the delay feedback strength passes through the threshold value given by $\eta\tau = -1$, localized patterns start to move spontaneously in an arbitrary direction. This is due to the isotropy of space (x, y). Example of 1D and 2D moving patterns consisting of one or two bounded cavity solitons are illustrated in Fig. 6 and 7, respectively. When two cavity solitons are separated initially by a distance of order of the wavelength associated with the modulational instability, they repeal each other, and, therefore, start to move with equal but opposite velocities as shown in Fig. 8. Localized patterns consisting

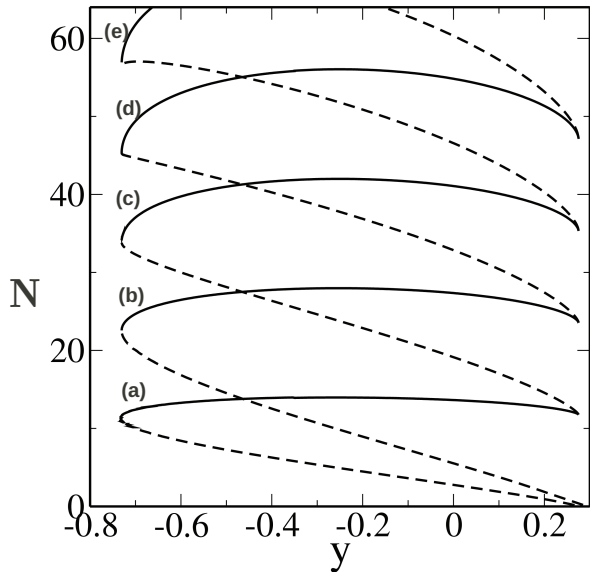

Figure 5: Snaking bifurcation diagram of Eq. (5) showing two inter-weaved snaking curves: the branches (a), (b), (c), (d), (e) correspond to 1, 2, 3, 4, 5 cavity solitons, respectively (see Fig. 3). The full and the broken lines correspond, respectively, to stable and unstable localized branches of solutions. The parameters are $p = -0.7$, $d = -1.2$, $a = 0.75$, and $\tau = \eta = 0$.

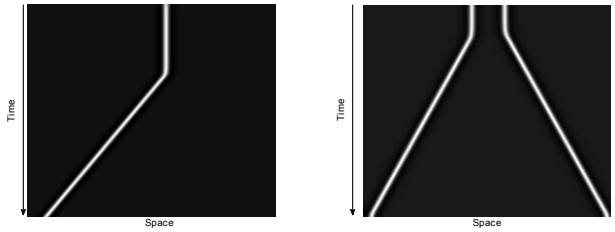

Figure 6: Space-time map of a moving cavity solitons solution of Eq. (5) in 1D. (left) single cavity solitons (right) two cavity soltions. Parameters are $p = -0.9$, $d = -1.5$, $a = 0.75$, $y = -0.5$, $\eta = -0.15$, and $\tau = 15$..

of a larger number of cavity solitons exhibit a similar behavior (see Fig. 9) The results shown in Figs. 6-9 have been obtained by numerical simulations of the generalized delayed Swift-Hohenberg equation (5) with periodic boundary conditions.

4.2 Drift instability threshold and the velocity of the moving cavity soliton

We have shown that below the drift instability threshold the modified SH equation Eq. (5) admits stationary localized patterns involving either an odd or an even number of cavity solitons. In this section, we discuss spontaneous motion of cavity solitons induced by the delayed feedback. We calculate the threshold value of the feedback strength above which cavity solitons start to move in an arbitrary direction and derive an expression for the velocity of the cavity soliton.

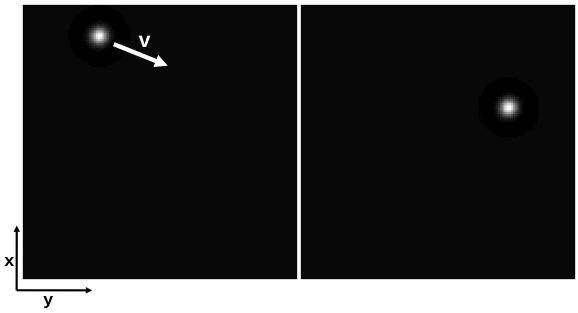

Figure 7: Moving 2D cavity soliton solution of Eq. (5). Parameters are the same as in Fig. (6). The size of the system is 128×128.

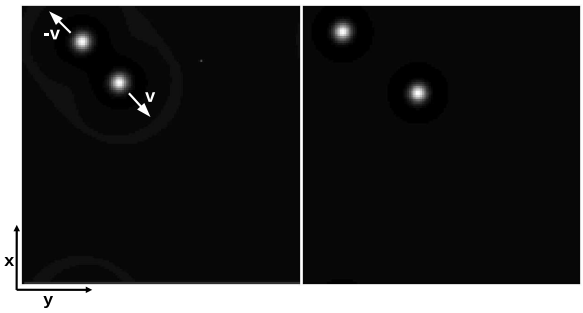

Figure 8: Moving 2D cavity soliton solution of Eq. (5). Parameters are the same as in Fig. (6). The size of the system is 128×128.

By presenting the results of numerical simulations of the full dynamical model Eqs. (1) and (2) we demonstrate that the existence of 2D moving cavity solitons is not restricted to the nascent bistability regime but can also occur far from that regime.

Analytical expression for the drift instability threshold was derived in Ref. [26] in the case of variational Swift-Hoheneberg equation with delay describing the passive nonlinear cavity. Let us first rewrite Eq. (5) in the form

$$\begin{aligned} \partial_t u &= y - u(p' + u^2) + \eta(u(t-\tau) - u) \\ &+ (d - \frac{5u}{2})\nabla_\perp^2 u - \frac{(1-\alpha^2)}{4\alpha^2}\nabla_\perp^4 u - 2(\nabla_\perp u)^2, \end{aligned} \tag{11}$$

with $p' = p - \eta$. We will assume that Eq. (11) without the term $\eta(u(t-\tau) - u)$ has a stable stationary radially symmetric soliton solution $u = u_0(|\mathbf{r}|)$. Stability of this solution means all the

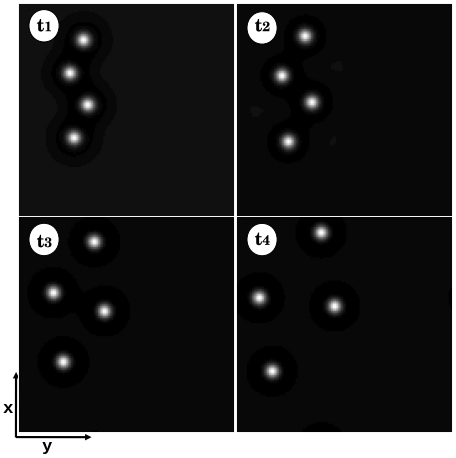

Figure 9: Moving 2D localizes pattern formed by four cavity solitons. Time sequence ($t_1 < t_2 < t_3 < t_4$) of the amplitude of the intracavity field solutions of the generalized delayed Swift-Hohenberg Eq. (5). Parameters are the same as in Fig. (8).

solutions Λ the eigenvalue problem

$$\mathcal{L}_\perp \phi = \Lambda \phi, \tag{12}$$

with self-adjoint operator

$$\mathcal{L}_\perp = -\left(p' + 3u_0^2 + \frac{5}{2}\nabla_\perp^2 u_0\right) + (d - \frac{5u_0}{2})\nabla_\perp^2 - a\nabla_\perp^4,$$

are real and negative except for a pair of zero eigenvalues corresponding to the translational invariance of Eq. (11), $\Lambda_{1,2} = 0$. Since the term $\eta(u(t-\tau) - u)$ vanishes at any stationary solution, the stationary soliton $u_0(|\mathbf{r}|)$ is also a solution of Eq. (11) with $\eta \neq 0$. Let us substitute slightly perturbed soliton solution $u(\mathbf{r}, t) = u_0(|\mathbf{r}|) + \phi e^{\mu t}$ into Eq. (11). Then linearizing it with respect to small perturbation ϕ we obtain:

$$\mathcal{L}_\perp \phi = \left[\mu + \eta\left(1 - e^{\mu\tau}\right)\right]\phi. \tag{13}$$

From Eqs.(12) and (13) we see that for $\eta \neq 0$ the stability of cavity soliton solution u_0 requires that the real parts of all the solutions μ of the equation

$$\mu + (1 - e^{\mu\tau})\eta = \Lambda, \tag{14}$$

must be non-positive for all Λ satisfying Eq. (12). In particular, for the 2-fold degenerate eigenvalue $\Lambda_{1,2} = 0$, assuming that $|\mu| \ll 1$ and expanding Eq. (14) up to the second order terms in μ we get two real solutions

$$\mu_{1,2} = \frac{2(\eta\tau + 1)}{\eta\tau^2}, \mu_{3,4} = 0, \tag{15}$$

where zero solutions $\mu_{3,4}$ are associated with the translational symmetry of the model equations and $\mu_{1,2}$ change their sign at the drift instability point $\eta\tau = -1$. At this point, where Eq. (14)

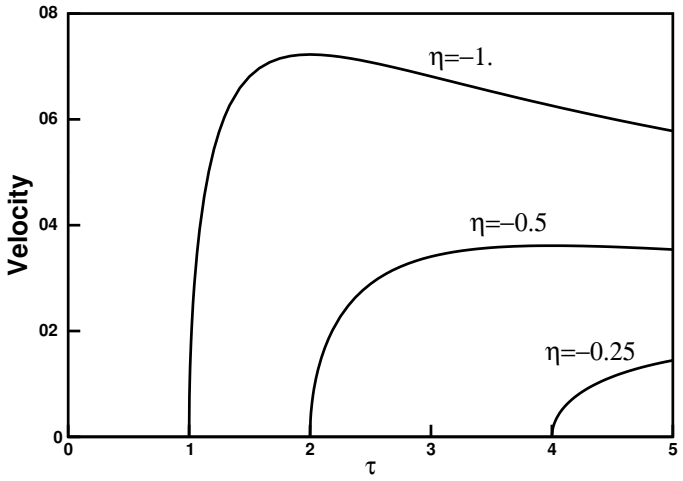

Figure 10: Velocity of moving cavity soliton as a function of the time delay τ for different values of the delayed feedback strength η.

has four-fold degenerate solution $\mu_{1,2,3,4} = 0$, stationary soliton solution looses stability and uniformly moving soliton solution bifurcates from the stationary one. According to Eq. (15) the stationary soliton is stable for $-1/\tau < \eta < 0$ and becomes unstable for $\eta\tau < -1$. The velocity of the moving single cavity soliton can be estimated by performing an expansion in terms a small parameter ζ which measures the distance from the drift instability threshold, $\eta\tau = -1 - \zeta^2$. Let us look for a solution of Eq. (11) in the form of uniformly moving cavity soliton:

$$u(\mathbf{r}, t) = u_0(\mathbf{R}) + \zeta^3 \delta u(\mathbf{R}) + ..., \quad \mathbf{R} = \mathbf{r} - \mathbf{v}t,$$

where u_0 is the stationary soliton solution evaluated at the drift instability point, $\mathbf{v} = \zeta\mathbf{V}$ is the soliton velocity, and δu is the correction to the soliton shape due to its motion. Plugging this expression in Eq. (5), using the expansion, $u_0(\mathbf{R} - \zeta V\tau) = u_0(\mathbf{R}) - \zeta V\tau u_1(\mathbf{R}) + (\zeta V\tau)^2 u_2(\mathbf{R})/2 - (\zeta V\tau)^3 u_3(\mathbf{R})/6 + ...$, where $V = |\mathbf{V}|$ and $u_p = (\mathbf{V} \cdot \nabla_\perp u_{p-1})/V$ $(p = 1, 2, 3, 4)$, and collecting third order in ζ, we obtain the following inhomogeneous problem

$$\mathcal{L}_\perp \delta u = -V u_1 + \frac{\eta}{6}(V\tau)^3 u_3. \tag{16}$$

According to the solvability condition, the right-hand side of this equation should to be orthogonal to the translational neutral modes $\phi_{x,y} = \partial_x u_0, \partial_y u_0$. By multiplying Eq. (16) with the linear combination of these modes $\mathbf{V} \cdot \nabla_\perp u_0/V \equiv u_1$ and integrating over 2D space, we obtain the equation for the cavity soliton velocity:

$$V\left(\int_{-\infty}^{+\infty} u_1^2 dxdy - \frac{\eta}{6} V^2\tau^3 \int_{-\infty}^{+\infty} u_1 u_3 dxdy\right) = 0. \tag{17}$$

Nontrivial solution of Eq. (17) is given by

$$v = \zeta V = \frac{Q}{\tau}\sqrt{-(1+\eta\tau)}, \quad \text{with} \quad Q = \sqrt{6\frac{\int_{-\infty}^{+\infty} u_1^2 dxdy}{\int_{-\infty}^{+\infty} u_2^2 dxdy}}, \tag{18}$$

where the relation $\int_{-\infty}^{+\infty} u_1 u_3 dxdy = -\int_{-\infty}^{+\infty} u_2^2 dxdy$ was used obtained by integration by parts. The expression for the soliton velocity (18) coincides with that obtained earlier for the case of variational Swift-Hohenberg equation [26, 27], which describes a driven passive nonlinear cavity filled with two-level atoms. This expression is valid not only for a single cavity soliton but also for any localized patters. The spatial form of the pattern affects only the factor Q in Eq. (18), which can be calculated numerically. In particular, for the parameter values $y = -0.35$, $p = -0.7$, $d = -1.2$, $a = 0.75$, we obtain $Q = 1.44$. The dependence of the soliton velocity on the time delay calculated using Eq. (18) is plotted for a fixed value of the feedback strength in Fig. 4.2. It is seen that the curve of the velocity has a maximum at $\tau = -2/\eta$, which corresponds to the maximal velocity $v_{max} = -Q\eta/2$.

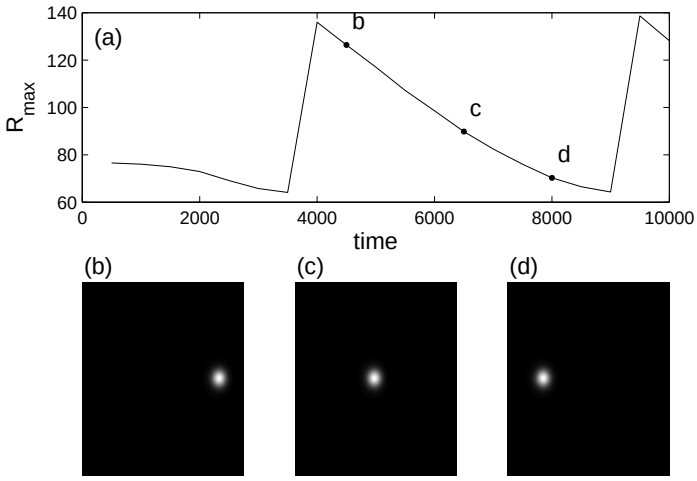

Figure 11: Time evolution of the spatially localized 2D solution $|E(x, y, t)|^2$ of Eqs. (1)-(2). (a) Time-evolution of the radius-vector R_{max} of the peak of the cavity soliton. (b), (c) and (d) Snapshots of the optical power distribution at the points indicated in (a). The parameter values are: $\eta = 0$, $\theta = -2$, $\alpha = 5$, $C = 0.45$, $I = 2$ and $\gamma = 0.05$, $E_i = 0.8$. The feedback strength and phase are given by $\eta = 0.1$ and $\xi = 3$, respectively.

Moving cavity solitons can be observed not only in the nascent optical bistability regime, but also far away from this regime. This is illustrated by Fig. 11, which was obtained by numerical integration of model Eqs. (1) and (2) using the Runge-Kutta method together with the fast Fourier transform. The boundary conditions were periodic in transverse directions. It is seen from Fig. 11 that a single cavity soliton exhibits a motion in an arbitrary direction in the (x, y) plane due to the presence of delayed feedback. Noteworthy, that in the absence of delayed feedback, cavity solitons were observed experimentally in broad area VCSELs both below [42, 7] and above [43] the lasing threshold.

5 Conclusions and perspectives

In conclusion, we have shown that close to the nascent bistability threshold, the space-time dynamics of a broad area Vertical-Cavity Surface-Emitting Lasers (VCSEL) operating below the lasing threshold and subject to optical injection is described by a generalized delayed Swift-Hohenberg equation. We show that in one transverse dimension, stationary cavity solitons exhibit a clustering behavior in the pinning range of parameters, where spatially homogeneous and periodic solutions are both linearly stable. In this range we construct a snaking bifurcation diagram associated with stationary cavity solitons. We demonstrate that one and two-dimensional cavity solitons exhibit a drift instability leading a spontaneous motion in an arbitrary direction. We estimate the threshold of this instability and the velocity of the moving cavity solitons. In two dimensions, the motion of two cavity solitons is studied numerically. Finally, numerical simulations of the original model (1) and (2) show that the described behavior is not limited to the nascent optical bistability regime but can also exist far away from this regime.

References

[1] M. Tlidi, M. Taki, and T. Kolokolnikov, Ïntroduction: Dissipative localized structures in extended systems", Chaos, **17**, 037101 (2007).

[2] N. Akhmediev and A. Ankiewicz "Dissipative Solitons: From Optics to Biology and Medicine"(Springer-Verlag, Berlin, Heidelberg, 2008).

[3] T. Ackemann, W.J. Firth, and G.L. Oppo, Advances in Atomic Molecular and Optical Physics, **57**, 323 (2009).

[4] O. Descalzi, M.G. Clerc, S. Residori, and G. Assanto, "Localized States in Physics: Solitons and Patterns"(Springer, 2010).

[5] H. G. Purwins, H.U. Bodeker, and S. Amiranashvili, "Dissipative solitons", Advances in Physics, **59**, 485 (2010).

[6] V.B. Taranenko, K. Staliunas, and C.O. Weiss, Phys. Rev. A **56**, 1582 (1997); V.B. Taranenko, K. Staliunas, and C.O. Weiss, Phys. Rev. Lett. **81**, 2236 (1998)

[7] S. Barland et al., Nature **419**, 699 (2002).

[8] X. Hachair et al., Phys. Rev. A **72**, 013815 (2005).

[9] U. Bortolozzo, L. Pastur, P.L. Ramazza, M. Tlidi, and G. Kozyreff, Phys. Rev. Lett. **93**, 253901 (2004); M.G. Clerc, A. Petrossian, and S. Residori, Phys. Rev. E **71**, 015205 (2005); S. Residori et al., J. Opt. B: Quantum Semiclass. Opt. **6**, S169 (2004).

[10] D. Bajoni et al., Phys. Rev. Lett. **101**, 266402 (2008).

[11] P. Genevet, S. Barland, M. Giudici, and J.R. Tredicce, Phys. Rev. Lett. **101**, 123905 (2008).

[12] X. Hachair, G. Tissoni, H. Thienpont, and K. Panajotov, Phys. Rev. A **79**, 011801(R) (2009).

[13] M. Tlidi, P. Mandel, and R. Lefever, Phys. Rev. Lett. **73**, 640 (1994); A.J. Scroggie et al., Chaos, Solitons and Fractals **4**, 1323 (1994); A.G. Vladimirov, J.M. McSloy, D.V. Skryabin, and W.J. Firth, Phys. Rev. E **65**, 046606 (2002); M. Tlidi, A.G. Vladimirov, and P. Mandel, IEEE J. Quant. Electron. **39**, 216 (2003).

[14] A.G. Vladimirov, R. Lefever, and M. Tlidi, Phys. Rev. A **84**, 043848 (2011).

[15] N.N. Rosanov, S.V. Fedorov, and A.N. Shatsev, Phys. Rev. Lett. **95**, 053903 (2005); N. A. Veretenov, N. N. Rosanov, and S.V. Fedorov, Journal Optical and Quantum Electronics, **40**, 253 (2008).

[16] C.O. Weiss, H.R.Telle, K. Staliunas, and M. Brambilla, Phys. Rev. A **47**, R1616 (1993).

[17] S. V. Fedorov, A.G. Vladimirov, G.V. Khodova, and N.N. Rosanov, Phys. Rev. E **61**, 5814 (2000).

[18] S.V. Gurevich, H.U. Bödeker, A.S. Moskalenko, A.W. Liehr, and H.-G. Purwins, Physica D **199**, 115 (2004).

[19] D. Turaev, M. Radziunas, and A.G. Vladimirov, Phys. Rev. E **77**, 065201(R) (2008).

[20] P. Coullet, J. Lega, B. Houchmanzadeh, and J. Lajzerowicz, Phys. Rev. Lett. **65**, 1352 (1990).

[21] D. Michaelis, U. Peschel, F. Lederer, D.V. Skryabin, and W.J. Firth, Phys. Rev. E **63**, 066602 (2001).

[22] K. Staliunas and V.J. Sanchez-Morcillo, Phys. Rev. E **72**, 016203 (2005).

[23] P.L. Ramazza, S. Ducci, and F.T. Arecchi, Phys. Rev. Lett. **81**, 4128 (1998); E. Louvergneaux, C. Szwaj, G. Agez, P. Glorieux, and M. Taki, Phys. Rev. Lett. **92**, 043901 (2004); F. Papoff and R. Zambrini, Phys. Rev. Lett. **94**, 243903 (2005); R. Zambrini and F. Papoff, Phys. Rev. Lett. **99**, 063907 (2007); R. Zambrini and F. Papoff Phys. Rev. E **73**, 016611 (2006); S. Coen, M. Tlidi, Ph. Emplit, and M. Haelterman, Phys. Rev. Lett. **83**, 2328 (1999).

[24] K. Staliunas and V.J. Sanchez-Morcillo, Phys. Rev. A **57**, 1454 (1998).

[25] M. Tlidi, P. Mandel, and M. Haelterman, Phys. Rev. E **56**, 6524 (1997); M. Tlidi and P. Mandel, Phys. Rev. A **59**, 2575(R) (1999).

[26] M. Tlidi, A.G. Vladimirov, D. Pieroux, and D. Turaev, Phys. Rev. Lett. **103**, 103904 (2009); M. Tlidi et al., Eur. Phys. J. D **59**, 59 (2010).

[27] S. V. Gurevich and R. Friedrich, Instabilities of localized structures in dissipative systems with delayed feedback, arXiv:1206.7059 (2012).

Phys. Rev. Lett. **103**, 103904 (2009); M. Tlidi et al., Eur. Phys. J. D **59**, 59 (2010).

[28] Y. Tanguy, T. Ackemann, W.J. Firth, and R. Jager, Phys. Rev. Lett. **100**, 013907 (2008).

[29] P.V. Paulau, D. Gomila, T. Ackemann, N.A. Loiko, and W.J. Firth, Phys. Rev. E **78**, 016212 (2008).

[30] P.V. Paulau, D. Gomila, P. Colet, M. A. Matias, N.A. Loiko, and W.J. Firth, Phys. Rev. A **80**, 023808 (2009).

[31] P.V. Paulau, D. Gomila, P. Colet, N.A. Loiko, N.N. Rosanov, T. Ackemann, and W. J. Firth, Optics Express **18**, 8859 (2010).

[32] B.Y. Rubinstein, A.A. Nepomnyashchy, and A.A. Golovin, Phys. Rev. E **75**, 046213 (2007); Y. Kanevsky and A. A. Nepomnyashchy, Phys. Rev. E **76**, 066305 (2007); A. A. Golovin, Y. Kanevsky, and A. A. Nepomnyashchy, Phys. Rev. E **79**, 046218 (2009); S. Coombes and C.R. Laing, Physica D **238**, 264 (2009); P. Ghosh, Phys. Rev. E **84**, 016222 (2011).

[33] K. Panajotov and M. Tlidi, Eur. Phys. J. D **59**, 67 (2010).

[34] S. Barbay, X. Hachair, T. Elsass, I. Sagnes, and R. Kuszelewicz, Phys. Rev. Lett. **101**, 253902 (2008); F. Haudin, R.G. Rojas, U. Bortolozzo, S. Residori, and M.G. Clerc, Phys. Rev. Lett. **107**, 264101 (2011).

[35] L. Spinelli, G. Tissoni, M. Brambilla, F. Prati, and L. A. Lugiato, Phys. Rev. A **58**, 2542 (1998).

[36] G. Kozyreff, S.J. Chapman, and M. Tlidi, Phys. Rev. E **68**, 015201 (2003); C. Durniak et al., Phys. Rev. E **72**, 026607 (2005); G. Kozyreff and M. Tlidi, Chaos **17**, 037103 (2007).

[37] M. G. Clerc, A. Petrossian, and S. Residori, Phys. Rev. E **71**, 015205 (2005).

[38] E. Averlant, M. Tlidi, A.G. Vladimirov, H. Thienpont, and K. Panajotov (To be published).

[39] A.R. Campneys, Physica D **112**, 158 (1998); G.W. Hunt, G.J. Lord, and Champneys, Compt. Methods Appl. Mech. Eng. **170**, 239 (1999); P. Coullet, C. Riera, and C. Tresser, Phys. Rev. Lett. **84**, 3069 (2000).

[40] J. Burke and E. Knobloch, Chaos **17**, 037102 (2007); Y.-P. Ma, J. Burke and E. Knobloch, Physica D **239**, 1867 (2010); D.J.B. Lloyd, B. Sandstede, D. Avitabile, and A.R. Champneys, SIAM J. App. Dyn. Syst **7**, 1049 (2008); M. Tlidi and L. Gelens, Opt. Lett. **35**, 306 (2010).

[41] G. Kozyreff, M. Tlidi, A. Mussot, E. Louvergneaux, M. Taki, and A. G. Vladimirov Phys. Rev. Lett. **102**, 043905 (2009); M. Tlidi, P. Kockaert, and L. Gelens, Phys. Rev. A **84**, 013807 (2011).

[42] V.B. Taranenko, I. Ganne, R.J. Kuszelewicz, and C.O. Weiss, Phys. Rev. A **61**, 063818 (2000).

[43] X. Hachairet al., IEEE J. Sel. Top. Quant. Electr. **12**, 339 (2006).